



# INNOVATIVE SOLUTIONS FOR LOWERING THE CONVERSION COST OF STEEL IN ARC FURNACES<sup>1</sup>

Said Alameddine <sup>2</sup>  
Ben Bowman <sup>3</sup>  
Stefan Paege <sup>2</sup>  
Paul Stafford <sup>4</sup>

## Abstract

In their continuous quest to increase productivity steelmakers normally search for higher power even if it may come at the expense of increasing energy consumption. However, when the market demand shrinks, productivity loses its pre-eminence and more emphasis can be placed on reducing the conversion cost. A lower productivity can be considered if it is accompanied by a lower cost. In this presentation we will describe various operational modifications, supported by actual examples, which can reduce energy consumption. The topics we discuss are the following: Hot heel size: heat size optimization from an energy loss perspective; Arc voltage optimization during refining; The diminishing thermal equivalence of increasing oxygen input; Use of slag enhancers to improve foaming quality and reduce FeO loss; A way to define the optimum target for tapping temperature on a heat to heat basis; Reducing electrical losses in a compensation system such as the SVC; Additionally we will highlight the possible advantages of vertical lancing; Finally we suggest a composite water cooled/ refractory roof to reduce heat loss.

**Key words:** Energy losses; Reduction of SVC loss; Hot heel size and heat size optimization; Arc voltage optimisation during refining; Oxygen equivalence.

## SOLUÇÕES INOVADORAS PARA REDUÇÃO DO CUSTO DE TRANSFORMAÇÃO DO AÇO EM FORNOS ELÉTRICOS A ARCO

### Resumo

Na busca contínua para incrementar a produtividade dos fornos elétricos a arco, os fabricantes de aço normalmente optam por maiores níveis de potência, ainda que acompanhados pelo incremento do consumo energético. No entanto, num ambiente de mercado retraído, a produtividade do forno perde importância para a necessidade de redução do custo de operação. Neste trabalho descreveremos alternativas operacionais apoiadas em exemplos reais, admitindo certa perda de produtividade, que podem reduzir o consumo de energia e, portanto, do custo de produção no forno elétrico a arco.

<sup>1</sup> *Technical contribution to the 41<sup>th</sup> Steelmaking Seminar – International, May, 23<sup>rd</sup>-26<sup>th</sup> 2010, Resende, RJ, Brazil.*

<sup>2</sup> *GrafTech Switzerland S.A*

<sup>3</sup> *GrafTech International Inc. USA*

<sup>4</sup> *GrafTech UK Ltd.*



## INTRODUCTION

The 2 figures below show that only 50% of the energy input is used to melt the steel.

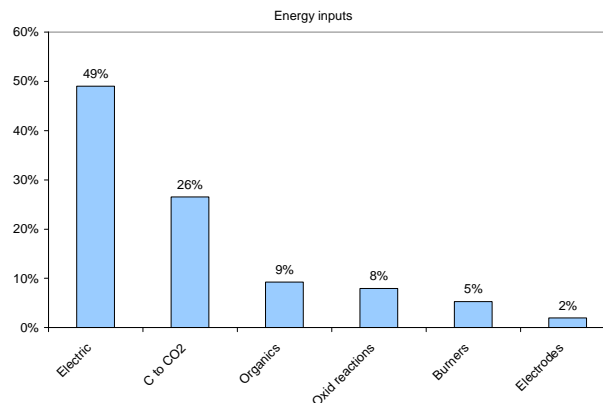


Figure 1: Typical energy inputs for 100% scrap.

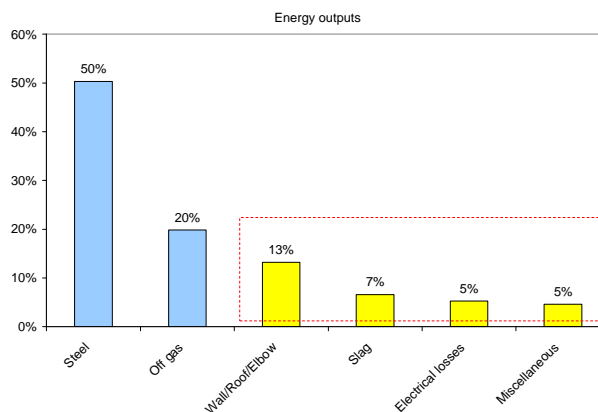


Figure 2: Typical energy outputs for 100% scrap.

In this paper we would like to consider how to reduce the energy costs, and will focus mainly on heat losses, heat transfer and consider a few items like oxygen thermal equivalence, slag chemistry, tapping temperature and the optimum use of the SVC to limit the energy bill.

## HOT HEEL SIZE

Few arc furnaces use a relatively large hot heel today, however, from a total energy perspective the selection of the optimum hot heel and heat sizes for a given furnace depends essentially on increasing the hot heel % vs. tapped liquid tonnes, the scrap density in use and ultimately the possibility to sacrifice the heat size to optimise the total energy requirement.

In our technical database usually hot heel size in % of the tapped liquid tonne ranges from 4 to 22% with an average around 11%. However Gottardi et al <sup>[1]</sup> mentioned recently that in one case a tall furnace using one basket charge was operating with a 30 to 42% hot heel, the total energy of this furnace was reported in the vicinity of 540 kWh/t according to our GrafTech total energy formula <sup>[3]</sup>. This is a good number for a high productivity furnace since our average based on numerous high productivity furnaces is about 580 kWh/liq.t (see Fig.3). That triggered the question of the



contribution of the furnace design (one basket charged) and the contribution of the hot heel.

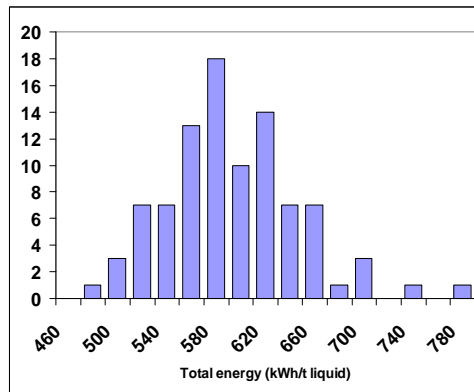


**Figure 3:** Total energy benchmark for high productivity furnaces using GrafTech formula <sup>[3]</sup>

We were then given the possibility to try to optimise the hot heel size on a high productivity furnace. Normalised total energy <sup>(4)</sup> for 3 hot heel levels of 6, 16 and 25%, were compared.

At this time this furnace was using various and inconsistent quantities of pig iron (5 to 20%) and HBI (0 to 5%). In particular the 25% hot heel test was run with no HBI, and pig iron ranging from 15 to 20%.

We attempted to take account of this charge inconsistency by normalising the total energy.<sup>4</sup> Results are presented in Table 1 and Figure 4.

**Table 1:** Hot heel influence on total energy requirement

Hot Heel in % on tapped liquid tonne	~ 6%	~ 16%	~ 25%
Mean (Normalised Total Energy <sup>4</sup> kWh/liq.t)	674	618	597
Std. error	6.4	3.5	4.9
Number of heats	120	400	80

While we acknowledge that the improvement in energy consumption may not be entirely due to the hot heel % we are confident that a significant portion of it is.

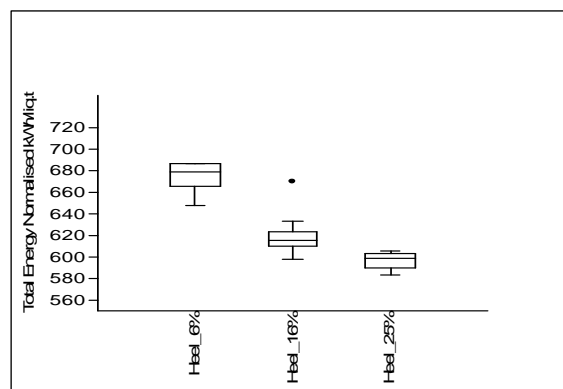


**Figure 4:** Hot heel influence on total energy requirement.

<sup>4</sup> Normalised total energy = total energy using GrafTech formula <sup>[3]</sup> and normalised to allow for the effects of temperature, fluxing quantity and the use of pig iron and DRI-HBI

It is worth mentioning that during the test of the ~ 25% hot heel, we experienced problems with un-melted scrap and temperature homogeneity that prevented us from selecting this level of the hot heel as an optimum.



This furnace is now targeting successfully a 16% hot heel.

We also want to point out two other advantages with the use of a larger hot heel. The first one is the positive contribution (probably due to a reduced vortex effect during tapping) to limit the amount of EAF slag carryover into the ladle. In this case the lower acidic oxides content makes the ladle slag less aggressive to basic refractory thereby providing a better protection to the slag line of the ladle. The second one is its ability to improve the arc stability earlier in the melt and hence a positive contribution to maximise the electrical energy input and reduce electrode columns oscillation.

## ARC VOLTAGE OPTIMIZATION DURING REFINING

Here we identify the arc voltage as an important parameter that influences the total energy requirement, both for AC and DC furnaces.

In a previous analysis<sup>[4]</sup> we have indicated higher total energy consumption for furnaces running very long arcs during the refining period. The slope of the correlation was 30 kWh / t per 100 V but because of a low correlation coefficient is not clearly defined.

Lower voltages however produce lower power so an optimum between energy consumption and power (productivity) needs to be found.

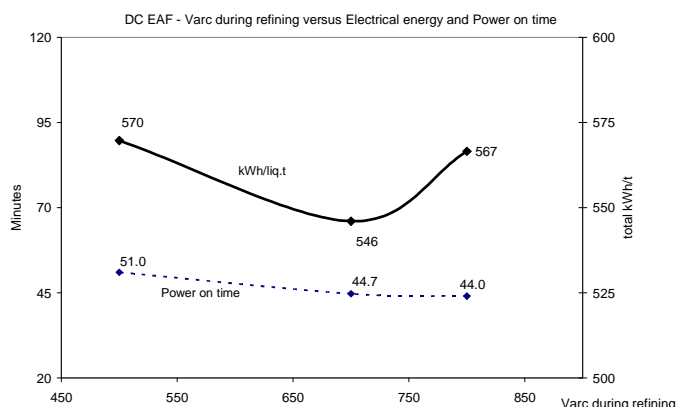


**Figure 5:** Example of the effect of arc voltage during refining on energy input requirement.

For a DC furnace we have measured a reduction of 10 kWh / t after reducing the arc voltage from 800 to 700 V during refining (see Figure 5).

We estimate that the arc voltage starts penalising the energy above 450 V for AC and 600 V for DC and operates at a rate of about 20 kWh / t per 100 V.

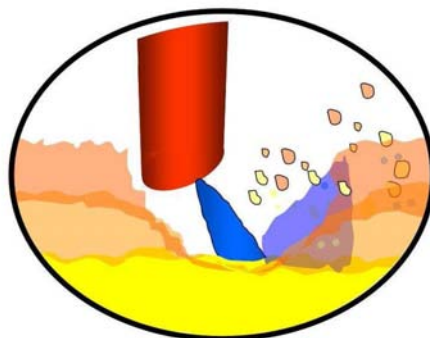


**Figure 6:** Arc efficiency of arc during refining.



Probably this effect is linked to the inability of the foaming slag to prevent increasing heat losses to the panels. Even though foaming slag depths are similar for AC and DC the lower limit on AC is probably a result of the arc blow-out and the higher “refractory index” (see Figure 6).

It is also evident that the effect of the arc voltage on the total energy requirement is even more significant for flat bath processes such as continuously charged DRI or scrap “Consteel”.

## THE DIMINISHING THERMAL EQUIVALENCE OF INCREASING OXYGEN INPUT

GrafTech’s EAF technical database as well as other sources listed below show a trend of diminishing electrical energy substitution with increased Oxygen input.

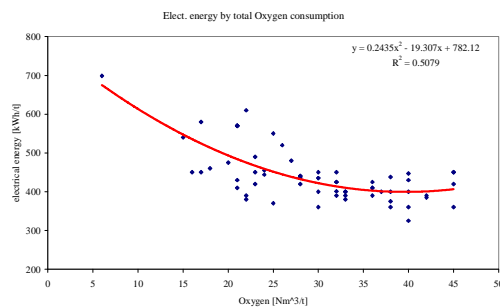


**Figure 7:** Electrical kWh/liq.t versus total oxygen from GrafTech’s technical database – every point represents a different furnace

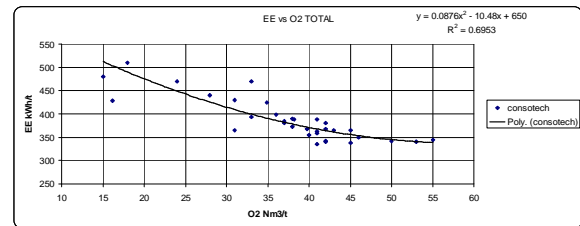


**Figure 8:** Electrical kWh/liq.t versus total oxygen from Concast – every point represents a different furnace<sup>[1]</sup>

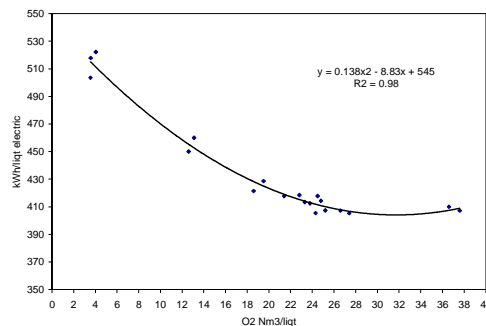
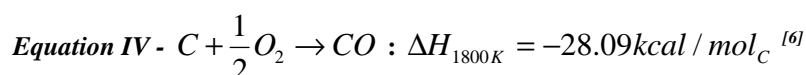
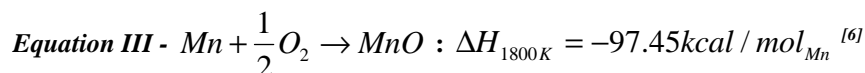
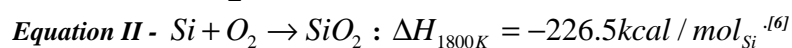
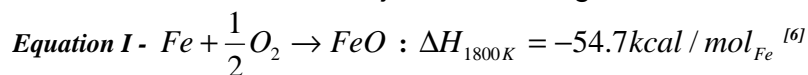


**Figure 9:** Electrical kWh/liq.t versus total oxygen – One furnace running with different rates of oxygen.<sup>[5]</sup>

In this chapter we will try to find the explanation for this observation. We start with the examination of the major contributing reactions that are:





We have shown the reaction enthalpy at 1800 K. But because furnace additions are normally cold they yield lower energy equivalence than indicated by the equations above, therefore, we need to subtract the energy necessary to heat the additions to furnace temperature.

**Equation VI** -  $\Delta H_{298to1800K} = 7.33kcal / mol_C$  Enthalpy increment for temperature change for C <sup>[6]</sup>

**Equation VII** -  $\Delta H_{298to1800K} = 12.36kcal / mol_{O_2}$  Enthalpy increment for temperature change for O<sub>2</sub> <sup>[6]</sup>

**Equation VIII** -  $\Delta H_{298to1800K} = 11.84kcal / mol_{CO}$  Enthalpy increment for temperature change for CO <sup>[6]</sup>

Based on the above reaction enthalpies, increment for temperature change enthalpies and free energy for carbon in solution in liquid iron we calculated the energy equivalences shown in Table 2, Figure 10 and Table 3.

**Table 2:** Energy equivalences in kWh/Nm<sup>3</sup> O<sub>2</sub>

kWh per Nm <sup>3</sup> of O <sub>2</sub>	Energy equivalence at 1527°C	Energy equivalence when all components are at 25°C (that is reaction enthalpy at 25°C)
for $C + \frac{1}{2}O_2 \rightarrow CO$ (exothermic reaction)		
O <sub>2</sub> Cold and Carbon Cold	1.51	
O <sub>2</sub> Cold and Carbon Hot (Carbon in solution in liquid iron)	3.59	
Commonly used figure		2.73

Free energy for carbon in solution in liquid steel is only considered above the eutectic temperature of carbon steel.

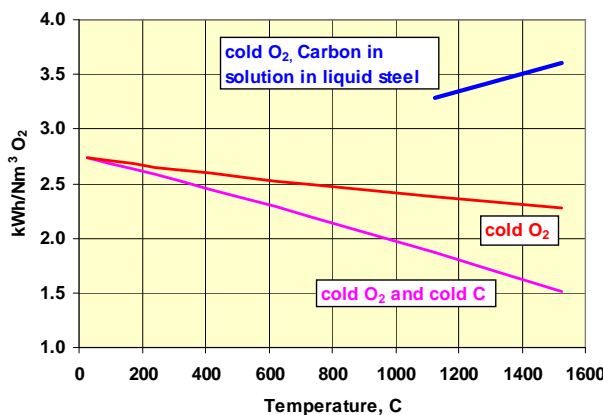


**Figure 10:** Temperature influence on  $C + \frac{1}{2}O_2 \rightarrow CO$  energy equivalence.

We consider a common 100% scrap operation producing carbon steel, hence we could assume 100kg of slag per tonne and 30% FeO in slag that is 30 kg of FeO per tonne. We comment that scrap may contain 30 kg/t of iron oxides and although there will be continuous reduction and oxidation reactions of iron oxides or iron during the heat, the net content of the iron oxide at the start (i.e. in scrap) and at the end (i.e. in the slag) is roughly the same.



**Table 3:** Energy equivalences in kWh/Nm<sup>3</sup> O<sub>2</sub>

Reactions	kWh per Nm <sup>3</sup> of O <sub>2</sub> With cold O <sub>2</sub> and reaction at 1527°C
$Si + O_2 \rightarrow SiO_2$	11.11
$Mn + \frac{1}{2}O_2 \rightarrow MnO$	9.47
$C + \frac{1}{2}O_2 \rightarrow CO$ Carbon in solution in liquid iron.	3.59
$C + \frac{1}{2}O_2 \rightarrow CO$ Added carbon considered cold	1.51
$Fe + \frac{1}{2}O_2 \rightarrow FeO$	5.03
	kWh per Nm <sup>3</sup> of O <sub>2</sub> With cold O <sub>2</sub> "Heat of combustion"
$CH_4 + 2O_2 \rightarrow CO_2 + 2H_2O$	5.25

Therefore we will consider only the Si, Mn and carbon in the steel reactions and will add FeO only if its end content significantly exceeds the iron oxide content in the scrap.

We should differentiate between the oxygen reactions in the EAF for purely metallurgical reasons and those deliberately triggered to input chemical energy.

The main metallurgical reactions are the oxidation of Si, Mn & C <sup>5</sup> according to the following table where we refer to a typical scrap analysis.

**Table 4:** Required oxygen and energy equivalences for metallurgical reactions

	avg. % in scrap <sup>6</sup>	O <sub>2</sub> <sup>7</sup> req. for full Oxidation [Nm <sup>3</sup> /t scrap]	energy generated <sup>8</sup> [kWh/t scrap]
Si "in scrap"	0.40	3.20	35.56
Mn "in scrap"	0.60	1.22	11.57
C "in scrap"	0.12	1.12	4.02
<b>Sum</b>		<b>5.55</b>	<b>51.16</b>

<sup>5</sup> Post combustion of carbon monoxide was not considered.

<sup>6</sup> Note for Carbon in scrap: 0.12% is the difference of 0.2% in average in the scrap & 0.08% in the liquid steel at tapping.

<sup>7</sup> Note for Oxygen: It is assumed, that this is always "cold", injected at ambient temperature that is.

<sup>8</sup> Note for energy generated: For Carbon we included the free energy of solution in liquid steel (see equation V).

These three metallurgical reactions return a thermal equivalence of approximately 9.22 kWh/Nm<sup>3</sup> of O<sub>2</sub>. This agrees quite closely with Inagaki et al, Figure 9.

Compared to the other reactions that are intended to bring an additional chemical energy this value is rather high. Therefore the full thermal equivalence of the oxygen in a given furnace depends on the proportional contribution of the metallurgical reactions (~ 9.22 kWh/Nm<sup>3</sup> O<sub>2</sub>) and the reactions that are intended to bring chemical energy (~ 5.25 kWh/ Nm<sup>3</sup> O<sub>2</sub> for CH<sub>4</sub> and ~ 1.51 kWh/ Nm<sup>3</sup> O<sub>2</sub> for cold carbon). It is also worth mentioning that metallurgical reactions have not only the highest thermal equivalence but also the highest efficiency since these reactions take place directly in the bath.



In the case of DRI operations, injected O<sub>2</sub> and carbon do not supply significant energy to the steel but allow the slag to foam better giving better protection to the refractories, improving the heat transfer, the energy requirement and enabling the use of longer arcs to improve power and productivity.

## USE OF SLAG ENHANCERS TO IMPROVE FOAMING QUALITY AND REDUCE FeO LOSS

Generally the control of the slag quality can optimise various parameters such as energy requirement, heat losses, arc length, productivity, nitrogen pick up, metallic yield and refractory wear in addition to its primary metallurgical purpose. All of these parameters, with the exception of the metallic yield and the refractory wear, are relative to the control of the foaming slag depth and its sustainability.

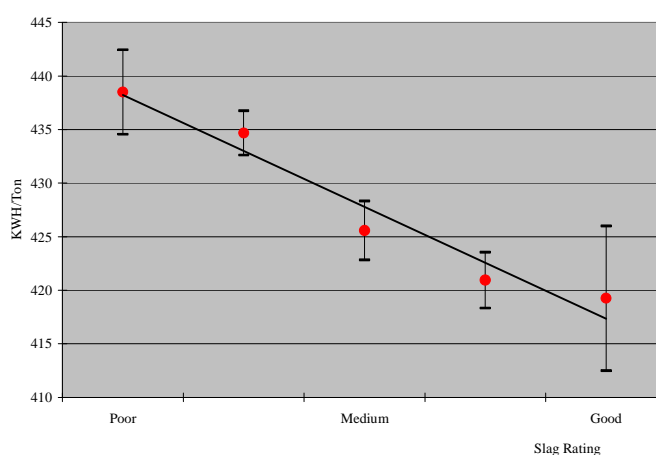


Figure 11: Energy consumption versus foaming slag quality<sup>[4]</sup>

We will first discuss the effect of the foaming slag depth.

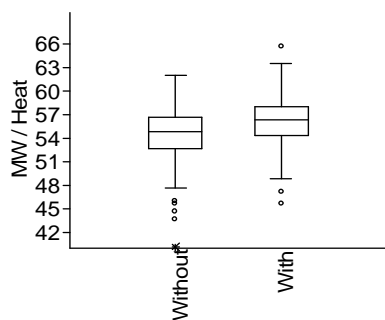
In a previous GrafTech paper Bowman et al.<sup>[4]</sup> discussed the effect of the quality of the foaming slag on the energy requirement (Figure 11).

Since then we have realised that the use of a foaming slag enhancer may contribute to the sustainability of the foaming slag depth and could improve meaningfully the average MW by reducing the arc instability that we measure as the % of the total harmonics distortion.

In the following discussion, all figures have been statistically tested using student t-test and population means were different with at least a confidence level of 95% with the exception of one that we will mention specifically.

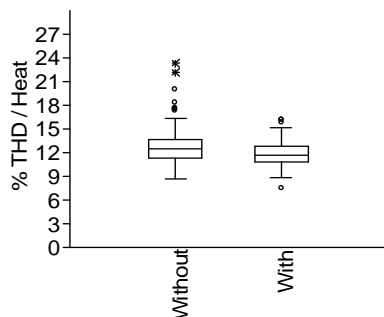
The figures reported are the result of the use of a foaming slag enhancer on a 90 MVA, 150 liquid tonne furnace. We report the statistics based on 123 heats using the foaming slag enhancer compared to 233 heats without. All of the heats using the same power programme.





MW average / Heat	Without	With
Mean:	54.4	56.0
N:	233	126

**Figure 12:** Average MW per heat without and with the use of the (MgO-carbon) foaming slag enhancer.



% THD / Heat	Without	With
Mean:	12.7	11.9
N:	233	126

**Figure 13:** Average % of total harmonics distortion per heat without and with the use of the (MgO-carbon) foaming slag enhancer.

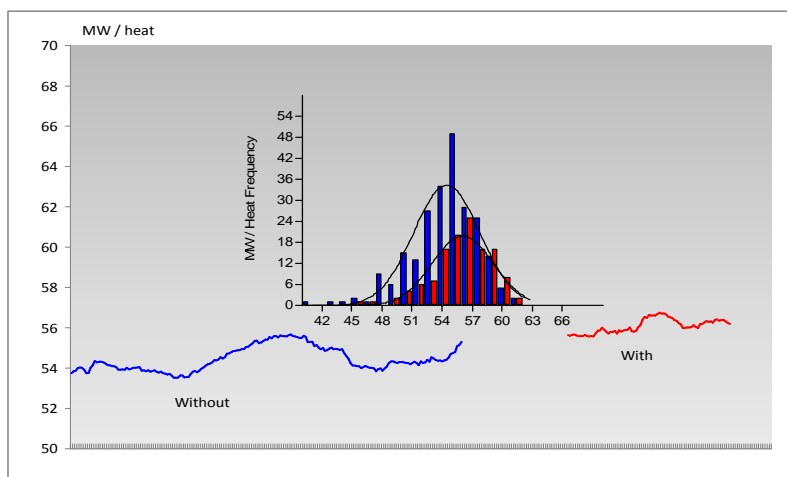


**Figure 14:** Moving average MW per heat without and with the use of the (MgO-carbon) foaming slag enhancer.

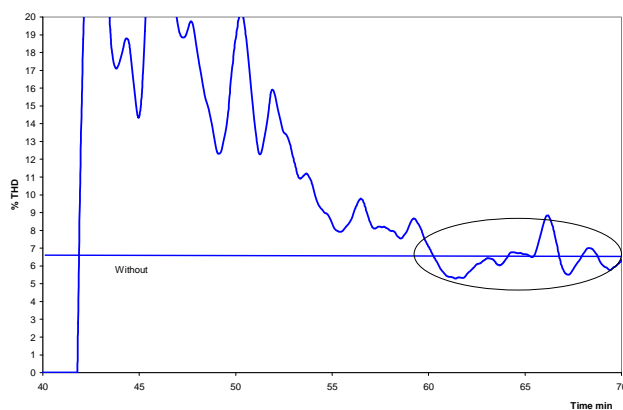


**Figure 15:** Example of a typical % of total harmonics distortion during refining prior to the use of the (MgO-carbon) foaming slag enhancer

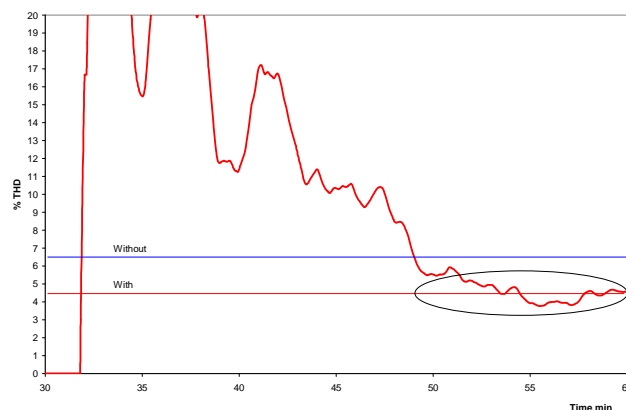


**Figure 16:** Example of a typical % of total harmonics distortion during refining with the use of the (MgO-carbon) foaming slag enhancer

Heat losses average as shown in the figure below are slightly lower with the use of the foaming slag enhancer. We were actually expecting some significant improvement due to a better coating effect. However the statistical t test shows no meaningful difference in this particular case.

**Table 5:** Heat losses in panels

Average panels losses / heat (MW)	Without	With	t-test
Mean:	2.65	2.53	t =1.41
N:	97	126	P (same) =16 %

Can we have a better foaming slag than the traditional “***lime – dololime - charged or injected carbon***” system?

We suspect that a properly designed slag enhancer might result in a faster dissolution of the MgO compared to MgO sourced by standard Dololime. In this case when close to saturation the slag enhancer yields a second phase that consists of a larger number of small MgO solid particles. Those particles have a lower surface tension than the unsaturated slag matrix and act as nuclei thereby improving the adsorption and retention of gas bubbles such as the CO.

Another possible advantage of a well covered arc by a foaming slag is the reduction of the nitrogen pick-up to the metal bath. Actually it is well known that high temperature of the arc causes N<sub>2</sub> cracking so the atomic nitrogen can penetrate the steel bath while molecular form N<sub>2</sub> can not. We assume that a confined arc in a foamy slag would yield less occurrence of nitrogen cracking near the arc. Actually some slag enhancer users report a better consistency of the nitrogen content in the steel but without documented evidence thus far.

Any steelmaking slag has a certain saturation point for MgO. Without any MgO fluxing the slag would be aggressive against the basic lining of the vessel. MgO fluxing will reduce the aggressiveness of the slag and the quicker the MgO is dissolved, the quicker the slag gets closer to or reaches the saturation point were the refractory erosion becomes minimal. One slag enhancer producer<sup>9</sup> claims that the MgO provided by his material is more active and dissolves much quicker than other MgO material sources such as crushed bricks or dololime.



**Figure 17:** Example of (MgO-Carbon) foaming slag enhance “Pro-Slag®<sup>[9]</sup> slag additive compound” briquettes - dimension “~ 40\*20\*20 mm”

<sup>9</sup> Pro-Slag is a registered trademark of ISM, Inc. of Wexford, PA.

This slag enhancer<sup>[9]</sup> contains in addition to the MgO, a certain percentage of carbon. In this case the carbon is included in the slag enhancer briquette (see Fig. 17) and hence available wherever the briquette disintegrates. Ideally this happens at the interface between the liquid steel bath and the slag and since the briquettes float evenly all over the liquid bath, the reactions with this carbon take place on a larger cross section compared to injected carbon.

This carbon then reacts with dissolved oxygen in the metal bath and reduces lower oxygen affinity oxides in the slag (mainly FeO). Both reactions create CO that supports slag foaming. The FeO reduction increases the metallic yield.

Injected carbon in the slag layer will create the same reactions; however several MgO-carbon slag enhancer users reported a lower total carbon demand and lower FeO content in the slag when using such material. In the following figures we discuss only the lower FeO content in the slag.

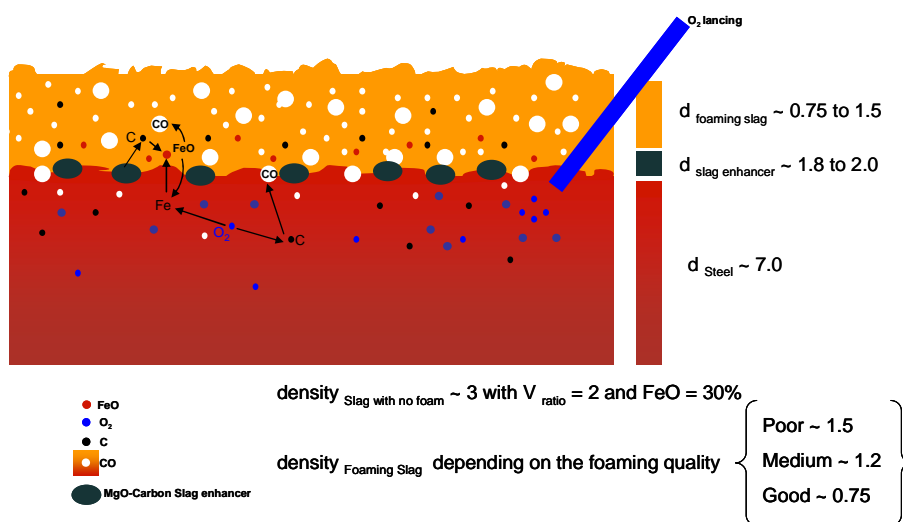


**Figure 18:** Claimed (MgO-carbon) foaming slag enhancer mechanism.

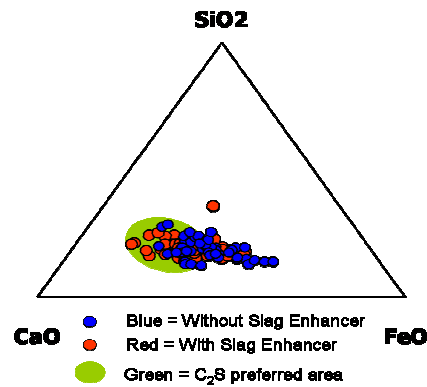
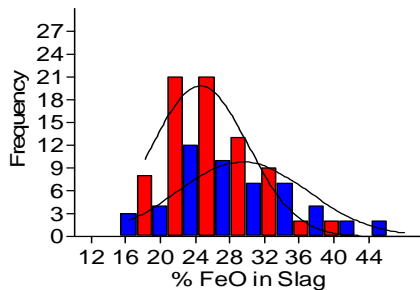


**Figure 19:** Example of the effect on FeO content in the slag with and without the use of (MgO-carbon) foaming slag enhancer.



% FeO in slag	Without	With
Mean:	29.4	24.5
N:	51	78

**Figure 20:** Example of the effect on FeO content in the slag with and without the use of (MgO-carbon) foaming slag enhancer

In the work of J. Liu et al in 2006 working on CaO/SiO<sub>2</sub>/Al<sub>2</sub>O<sub>3</sub> matrix with Al<sub>2</sub>O<sub>3</sub> =25%, it is reported that the dissolution rate of MgO particles is strongly influenced by the composition of the slag (starting MgO content if any) and by the temperature:

In this example, initially slag A contains no MgO and therefore the driving force for dissolution in slag A is high (solubility limit ± 12.5%). Slag B initially contains 7.3% MgO (solubility limit ± 11.5%) and therefore the driving force for dissolution in slag B is lower.

If local equilibrium is assumed at the particle/slag interface, the driving force for MgO dissolution is related to the concentration difference of MgO between the particle/slag interface and the bulk of the slag.

The concentration difference can be evaluated from the phase diagram, where it is given by the saturation limit. Both temperature and slag composition have marked effects on the dissolution rate of MgO through the change of this driving force.

The effects of temperature and slag composition can be explained with reference to the CaO–Al<sub>2</sub>O<sub>3</sub>–SiO<sub>2</sub>–MgO phase diagram. Liu et al <sup>[2]</sup> reported that ignoring the presence of minor constituents, the compositions of the slags A and B are shown in the CaO–Al<sub>2</sub>O<sub>3</sub> (25 mass%)–SiO<sub>2</sub>–MgO phase diagram (see Fig. 22). One can see that increasing the temperature from 1500 up to 1600°C enhances the saturation limit of MgO in slag A from about 12.5 – 19 mass%. Thus, the concentration difference is increased, and thus the driving force for MgO dissolution also.



Moreover, the increase in temperature accelerates the diffusion process. Therefore, higher temperatures lead to a faster dissolution rate and a decrease in dissolution time, as was observed. (see Fig 21).

As expected, increasing the initial MgO content in the slag (slag A → slag B) decreases the amount of MgO that can be dissolved thermodynamically (see Fig. 21). This leads to a decrease in the driving force for MgO dissolution as expressed by the concentration difference between the slag/particle interface and the bulk of the slag (the difference being reduced in this case from 12.5 to 4.2 mass %).

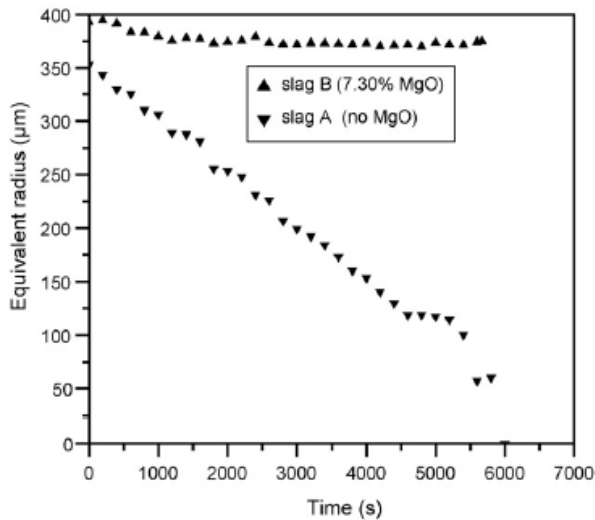


**Figure 21:** Effect of slag composition on the dissolution rate of MgO particles at 1500°C [2]

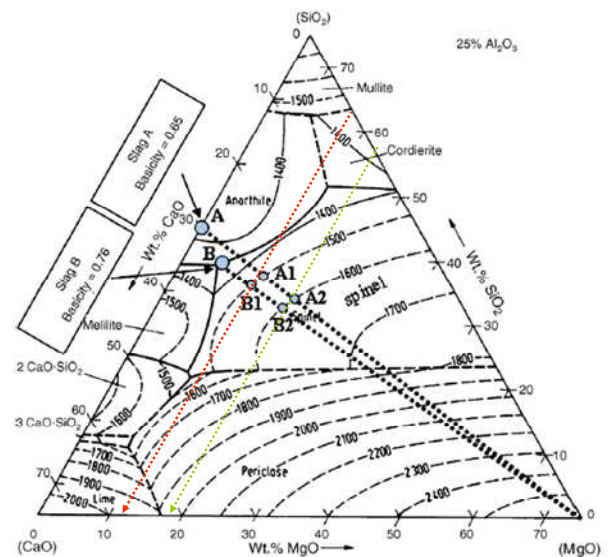


**Figure 22:** Liquidus projection of the CaO–Al<sub>2</sub>O<sub>3</sub>–SiO<sub>2</sub>–MgO phase diagram [2]

Considering the above, we question whether reaching the saturation limit of the MgO of a slag in order to limit the refractory erosion is necessary to give a positive economic result.

We propose to take into account the given slag concentration in MgO prior to the use of the slag enhancer, dolomite or crushed brick and to use it as a target MgO value when adding deliberately a source of MgO.

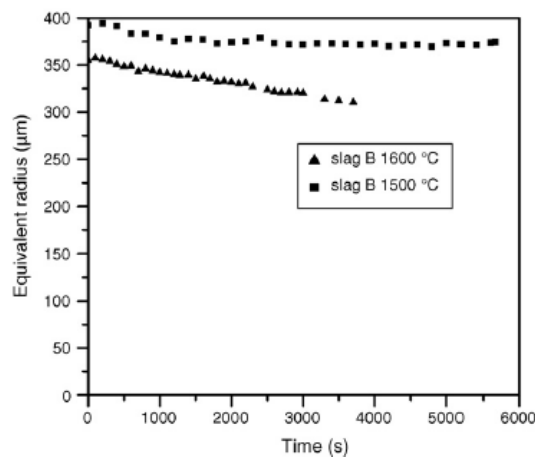


**Figure 23:** Dissolution curves of MgO in slag B [2]



We do not report any saving in refractory or gunning material as those numbers depend on the maintenance cycle and the practice of intermediate repair or gunning of individual furnaces.

However, generally the use of a slag enhancer yields superior results on those obtained with the use of common sources of MgO such as raw magnesite, dololime and or crushed MgO bricks.

## OPTIMUM TARGET FOR TAPPING TEMPERATURE ON A HEAT TO HEAT BASIS

Some steelmakers tend to set their tapping temperature rather on the high side to accommodate any logistical problem with the continuous caster. In other words they create deliberately a liquid buffer between the EAF and the continuous caster. In such a case it becomes important to manage the tapping temperature according to the estimated delay that will take place.

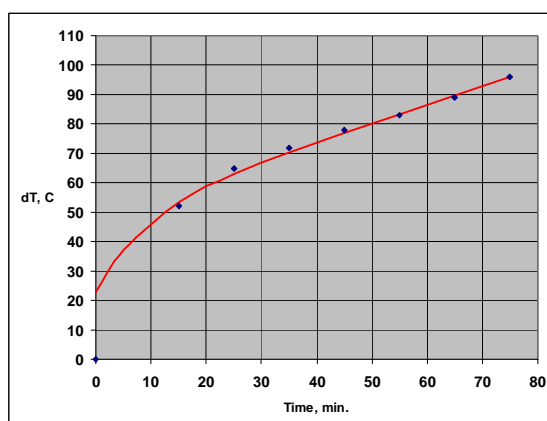


Figure 24: Temperature losses against time in a 100t ladle.

In one case we have analysed the liquid steel temperature losses against time in the ladle for 1000 heats (see Fig. 24).

Although the standard deviation around each point was high and stable  $\sim 20^{\circ}\text{C}$ , we have been then able to reduce in this case by more than  $10^{\circ}\text{C}$  the tapping temperature in the EAF and obtain a reduction of 5 to 7 kWh/t.

## REDUCING ELECTRICAL LOSSES IN A COMPENSATION SYSTEM SUCH AS THE SVC

According to two suppliers of flicker correction systems, pure losses in the SVC are usually around 0.5 to 0.7 MW per 100 MVAR. This should return for a 100 MVAR SVC, for a furnace that runs 50 MW, 50 MVAR, 70t/h and having a 50% Power ON, a maximum of 6 to 7 kWh/t as SVC losses.

In reality we can only measure losses that include the resistive line losses (proportional to  $\text{Amp}^2$ ).



## Complete furnace (AC)

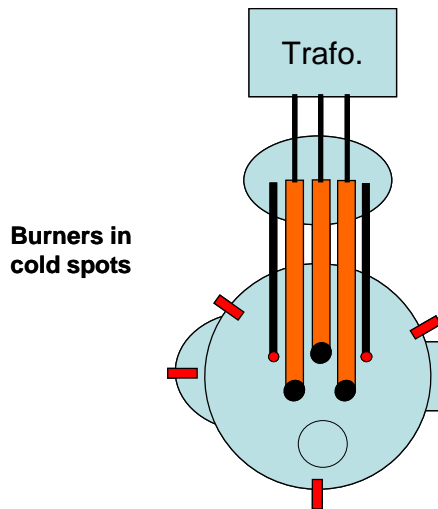


Figure 25: Line and SVC losses versus monthly production.

Line reactance measured by us is usually in the range 0.2 to 0.8 Ohm. (depending mainly on the distance between SVC and EAF transformer). This would return additional losses for 2000 amps average in the above example of 0.6 to 2.4 kWh/t. Hence measured losses (SVC + line) usually fall in the range of 6.5 to 9.5 kWh/t.

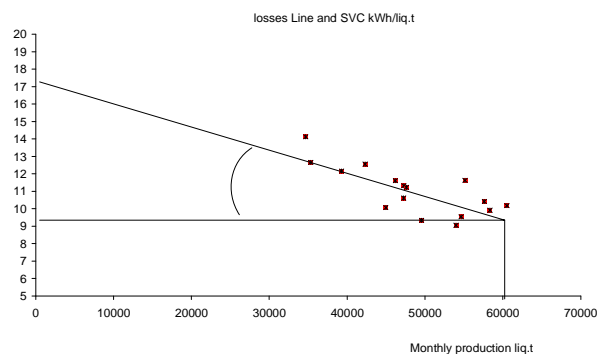


Figure 26: Possible design of an AC EAF with 2 vertical lances

Recently in 3 cases (operating at lower MW than original design) we have been able to turn off one of the filters of the SVC without affecting the flicker, resulting in reduced losses in the SVC up to 25%.

Our suggestion to introduce a new procedure [SVC off when EAF off for more than 2 hours & switch on SVC 10 min before start of the EAF] saved a further 25%.

Each time there is an SVC with a TCR (thyristor-controlled reactor) there will be losses mainly in the TCR. One supplier was proposing in the past the TyCap<sup>[8]</sup> (thyristor-controlled capacitors) solution that delivers lower flicker mitigation performance but results in lower electrical losses.



## POSSIBLE ADVANTAGES OF VERTICAL LANCING

We have noticed that one DC EAF working with 100% DRI and 3 vertical, moveable oxygen lances shows excellent performance figures compared to other similar DRI users. In our opinion the fact that the lances are vertical contributes to this good performance. Here we wanted to stand a bit outside of the conventional thinking and ask ourselves if vertical lancing could be realised in an AC EAF. Why should that not be considered even for scrap melting? Perhaps with a suitable lance regulation system the movement could follow the scrap descent just as electrodes do.

The use of vertical lancing may also permit to do what similar lances are doing at the end of the heat in the oxygen converters using nitrogen i.e. slag or splash coating of the sidewall. Convertors using this technique have extended life time of the refractory line of their vessel up to 15000 heats.

We believe that such a process could improve the panel's coating thus reducing the heat losses.

If successful this may trigger the question of the viability of a refractory wall that would be more or less comparable to the freeze lining technology used in submerged arc furnaces where high thermal conductivity refractories such as carbon bricks are used to protect the cooling panel while still freezing a layer of process material.

## COMPOSITE WATER COOLED/ REFRACTORY ROOF TO REDUCE HEAT LOSS

Historically the arc furnace had refractory walls and roofs prior to the introduction of the first water cooled panels in Japan in 1973. In Europe we have seen the first water cooled panels in 1975 and later on also water cooled roofs. Significantly all these developments took place prior to the introduction (again in Japan) of foaming slag techniques towards the end of the 1970s.

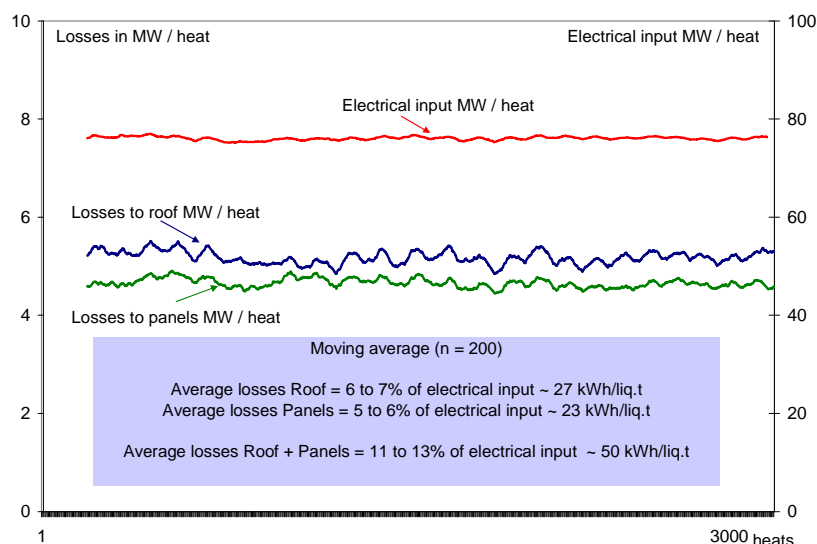


Figure 27: Relative importance of heat losses in panels and roof

So we ask - Is there a case for a return to refractory linings of walls and roof? Before the introduction of water cooled panels refractory lifetime was about 200 heats. At that time heats lasted 3 to 4 hours, so refractory lasted 600 to 800 hours **without foaming slag practice and without ladle furnaces**. Nowadays, with ladle





furnaces that reduce tapping temperature and foaming slag that reduces erosion of the walls and hot spot areas, what would be the refractory life? > 1000 hours = 1000 heats?

In the example given in Fig. 27, a 100% scrap melting EAF, 160liq.t, 120 MVA, the energy savings could be a good part of the current losses of the water cooled panels and roof (i.e. ~ 50 kWh/t).

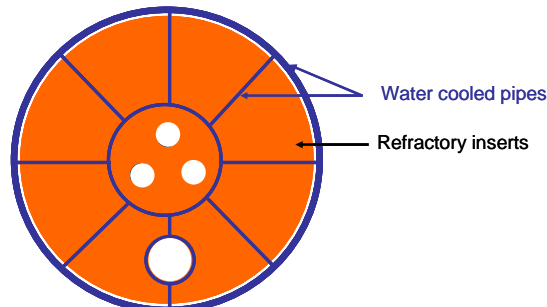


**Figure 28:** Possible composite roof. Steel structure with water cooled pipes and refractory fast changeable parts in the interstices

Today refractory is still involved in the delta; would it be possible to put more refractory in other parts of the roof in order to reduce the heat losses? In this case special consideration should be paid to the increased weight of the roof.

## CONCLUSION

In conclusion we discussed in this paper:

- The possibility to lower the energy demand of the EAF using a larger hot heel.
- The penalty for using long arcs during refining. 20kWh/t per 100V above 450 Varc for AC EAF or 650 Varc for DC EAF.
- The diminishing thermal equivalence of the increasing oxygen input (from 9.22 kWh/Nm<sup>3</sup> to 1.51 kWh/Nm<sup>3</sup>) to let the steelmaker decide the optimum proportion of the chemical and electrical energy depending on their cost structure and the productivity needs.
- The advantage of using slag enhancers to increase the power input during refining but also to improve the Fe yield and protect the refractory.
- The possibility of optimising the tapping temperature heat by heat for the steelmaker who needs to deal with inconsistent liquid buffer between the EAF and the continuous caster.
- Losses in the thyristor controlled reactor of the flicker reduction system (SVC) and explain how some of these losses can be reduced by disconnecting the SVC when the furnace is off, as well as the deactivation of part of the capacitor banks to fit with the power load of the furnace.

Finally, noting that about 50 kWh/t are lost in water cooled panels and roof, we discuss the possibility for steelmakers to consider vertical lancing, allowing slag coating (BOF practice) of side wall and a possible re-introduction of more refractory in roof and panels to reduce energy losses.



## REFERENCES

- 1 R. Gottardi, S. Miani, A. Partyka, “**A faster, more efficient EAF**”, European electrical steelmaking conference, Krakow, May. 2008.
- 2 J. Liu., M. Guo, P.T. Jones, F. Verhaeghe, B. Blanpain, P. Wollants, “**In situ observation of the direct and indirect dissolution of MgO particles in CaO–Al<sub>2</sub>O<sub>3</sub>–SiO<sub>2</sub>-based slags**”, Journal of the European Ceramic Society 27, 2007.
- 3 Adams, Alameddine, Bowman, Lugo, Paege, Stafford, “**Factors influencing the total energy consumption in arc furnaces**” 59<sup>th</sup> Electric Furnace & 19<sup>th</sup> Process technology update conference, Phoenix, 2001.
- 4 B. Bowman, N. Lugo and T.P. Wells, “**Influence of tap carbon and arc voltage on electrode and energy consumption**”, ISS, Electric Furnace Conference, Orlando, 2000, pp649-57.
- 5 E. Inagaki, K. Izumi and M. Ichikawa, “**Integrated oxygen enrichment control to attain maximum overall economy in steelmaking arc furnaces**” Proc. Electroheat Congress, Madrid, Oct. 1998, paper A6.2.
- 6 J.F. Elliott, **Physical chemistry of high temperature reactions**, Chapter 20, Electrical furnace steelmaking, ISS, 1985.
- 7 G.K. Sigworth and J.F. Elliott “**Met. Sci.**” 8 (1974):75.
- 8 Frank & Ivner; Tycap, “**Power factor correction equipment using thyristor controlled capacitors for arc furnaces**”, ASEA Journal 1973 no.6, p147 – 152.